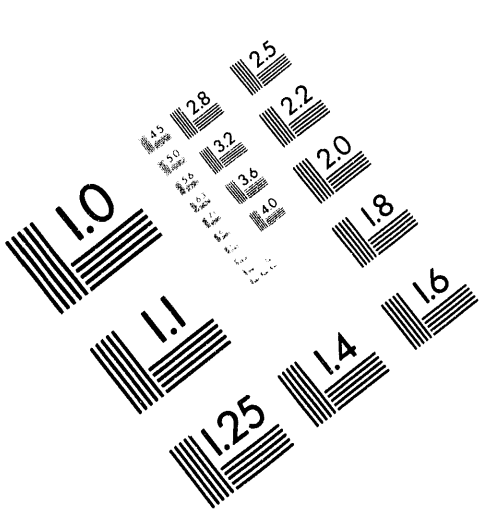

Association for Information and Image Management
1100 Wayne Avenue, Suite 1100
Silver Spring, Maryland 20910
301/587-8202

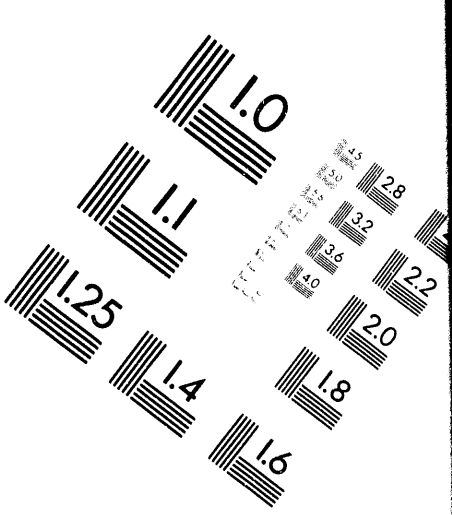

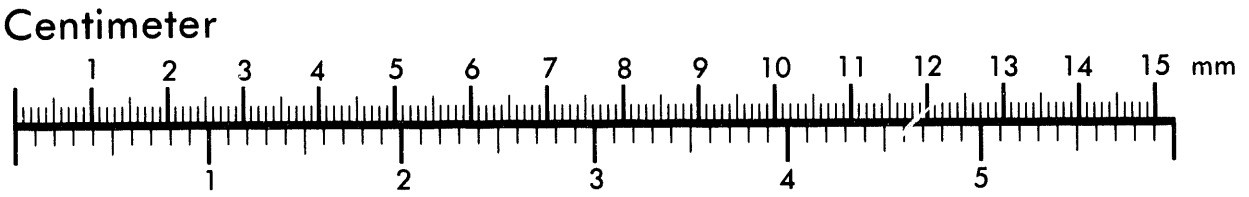

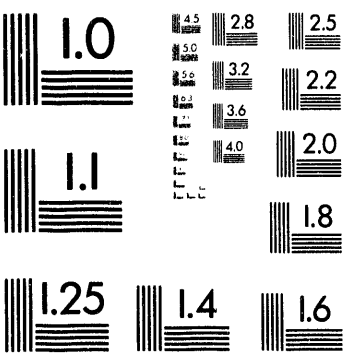

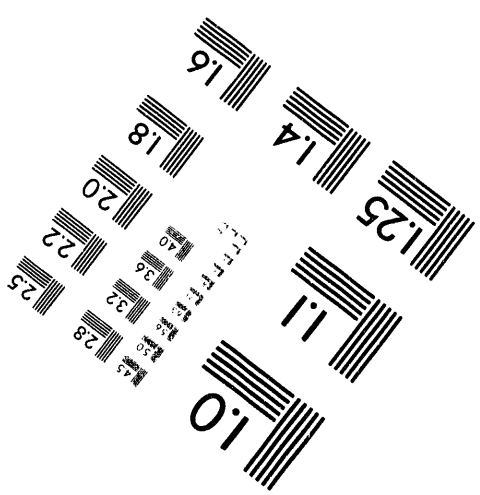

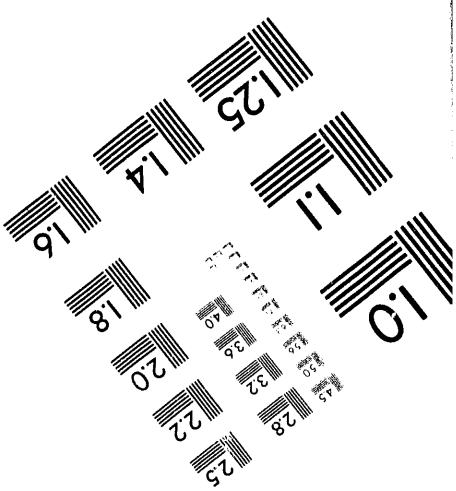

MANUFACTURED TO AIIM STANDARDS
BY APPLIED IMAGE, INC.

1 of 1

DOE/BC/14659--T8

CHARACTERIZATION OF NON-DARCY MULTIPHASE FLOW IN PETROLEUM BEARING FORMATIONS

DE-AC22-90BC14659

School of Petroleum & Geological Engineering
The University of Oklahoma

Contract Date: May 14, 1990

Anticipated Completion: May 13, 1993

Principal Investigators:

Ronald D. Evans
Faruk Civan

Contracting Officer's Representative:

Dr. Jerry Ham
Metairie Site Office

Annual Status Report - May 14, 1991 - May 13, 1992

OBJECTIVES

The objectives of this research are:

1. Develop a proper theoretical model for characterizing non-Darcy multi-phase flow in petroleum bearing formations.

2. Develop an experimental technique for measuring non-Darcy flow coefficients under multiphase flow at insitu reservoir conditions.

3. Develop dimensional consistent correlations to express the non-Darcy flow coefficient as a function of rock and fluid properties for consolidated and unconsolidated porous media.

The research accomplished during the period May 1991 - May 1992 focused upon theoretical and experimental studies of multiphase non-Darcy flow in porous media.

THEORETICAL STUDIES

During this annual reporting period effort was directed toward investigating relative permeability and capillary pressure effects under non-Darcy flow. A computational model was developed to simulate compressible, two phase non-Darcy flow under linear unsteady state displacement through laboratory cores. Using the basic measurements of flow rate, pressure differential, and fluid properties, relative permeabilities, capillary pressures and the non-Darcy flow coefficient were determined simultaneously using a non-linear optimization technique. The simulation was carried out using a block centered, single point upstream weighing of relative permeability. The boundary condition for imbibition displacement is as follows. At the inlet and outlet ends a reflection boundary condition was used for the pressures. However, there is no flow of the non-wetting phase until the outlet capillary pressure becomes zero. From that time, the outlet boundary condition is converted to the specified wetting phase pressure.

In order to test the numerical code, experimental data was obtained from results available in the open literature. The rock properties and operating conditions are given in Table 1. The relative permeability and capillary pressure curves are given in Fig. 1 and are representative of a strongly water-wet system.

Three different runs were conducted. In the first case the capillary pressure is assumed to be zero and results are compared with the analytical solution of the Buckley-Leverett model. As shown in Fig. 2, the breakthrough time for the analytical model is 448 sec. and for the numerical model it is 426 sec. The production history, pressure drop history and the saturation history profiles are given in Fig. 3, Fig. 4, and Fig. 5, respectively. The output summary of this run is given in Table 2 which gives information about the pore volume injection, water oil ratio, cumulative water production, cumulative fluid production, cumulative water injection, material balance, and capillary pressure curves. In the second and third cases, the capillary pressure and end-effect are included. The breakthrough time is 305 sec., without end-effect, and it is 407 sec.

Table 1: Core Properties and Operating conditions

k	= 1270 md	Injection Rate	= .006 cc/sec
o	= .249		= 1. cp
L	= 7.62 cm		= 10 cp
Area	= 5.06 cm^2	Pore Volume	= 9.6 cm^3
Swi	= .3		
Sor	= .2375		

Table 2: Production History, No Capillary Pressure case

Time (sec)	Por vol. Inj.	WOR	Wp (cc)	Np+Wp (cc)	Wi (cc)	Material Balance	P (psi)
0.0	0.0000	0.0000	0.0000	0.0000	0.0000	0.0000	0.0000
1.0	0.0006	0.0000	0.0000	0.0000	0.0060	0.0000	0.0000
2.0	0.0012	0.0000	0.0000	0.0060	0.0120	0.0000	0.0306
100.0	0.0609	0.0000	0.0000	0.5932	0.6000	-0.0001	0.0311
200.0	0.1219	0.0000	0.0000	1.1927	1.2000	-0.0002	0.0301
300.0	0.1828	0.0000	0.0000	1.7907	1.8000	-0.0005	0.0293
400.0	0.2437	0.0000	0.0000	2.3925	2.4000	-0.0003	0.0300
500.0	0.3047	1.8442	0.1279	2.9947	3.0000	0.0000	0.0108
1000.0	0.6091	3.2671	2.4094	5.9935	6.0000	-0.0006	0.0051
1500.0	0.9139	3.3289	4.7131	8.9957	9.0000	0.0001	0.0098
2000.0	1.2102	3.4433	6.9589	11.9088	11.9998	-0.0174	0.0023
3500.0	2.1295	3.5314	14.0167	20.9516	20.9999	-0.0031	0.0005

Table 3: Production History, With Capillary Pressure case

Time (sec)	Por vol. Inj.	WOR	Wp (cc)	Np+Wp (cc)	Wi (cc)	Material Balance	P (psi)
0.0	0.0000	0.0000	0.0000	0.0000	0.0000	0.0000	0.0000
1.0	0.0006	0.0000	0.0000	0.0000	0.0060	0.0000	0.0000
2.0	0.0012	0.0000	0.0000	0.0060	0.0120	0.0000	0.0306
100.0	0.0609	0.0000	0.0000	0.5932	0.6000	-0.0001	0.0311
200.0	0.1219	0.0000	0.0000	1.1928	1.2000	-0.0002	0.0304
300.0	0.1828	0.0024	0.0001	1.7938	1.8000	0.0000	0.0306
400.0	0.2437	1.0442	0.1610	2.3938	2.4000	0.0000	0.0150
500.0	0.3047	2.2917	0.5313	2.9938	3.0000	0.0000	0.0094
1000.0	0.6093	6.8848	2.9867	5.9938	6.0000	0.0000	0.0040
1500.0	0.9140	11.4124	5.6805	8.9938	9.0000	0.0000	0.0026
2000.0	1.2186	18.4202	8.4876	11.9938	11.9998	0.0002	0.0017
3500.0	2.1327	49.0988	17.2030	20.9938	20.9999	0.0000	0.0007

Table 3: Production History, With Capillary Pressure case

Time (sec)	Por vol. Inj.	WOR	Wp (cc)	Np+Wp (cc)	Wi (cc)	Material Balance	P (psi)
0.0	0.0000	0.0000	0.0000	0.0000	0.0000	0.0000	0.0000
1.0	0.0006	0.0000	0.0000	0.0000	0.0060	0.0000	0.0000
2.0	0.0012	0.0000	0.0000	0.0060	0.0120	0.0000	0.0306
100.0	0.0609	0.0000	0.0000	0.5932	0.6000	-0.0001	0.0311
200.0	0.1219	0.0000	0.0000	1.1928	1.2000	-0.0002	0.0304
300.0	0.1827	0.0000	0.0000	1.7835	1.8000	-0.0016	0.0256
400.0	0.2410	0.0000	0.0000	2.1732	2.4000	-0.0330	0.0412
500.0	0.3047	2.8626	0.3938	2.9984	3.0000	0.0000	0.8494
1000.0	0.6093	2.1219	2.3202	5.9984	6.0000	0.0000	1.6554
1500.0	0.9140	2.6318	4.4333	8.9983	9.0000	0.0001	1.0660
2000.0	1.2186	3.0073	6.6499	11.9984	11.9998	0.0004	0.7246
3500.0	2.1327	3.5494	13.5807	20.9984	20.9999	0.0004	0.3323

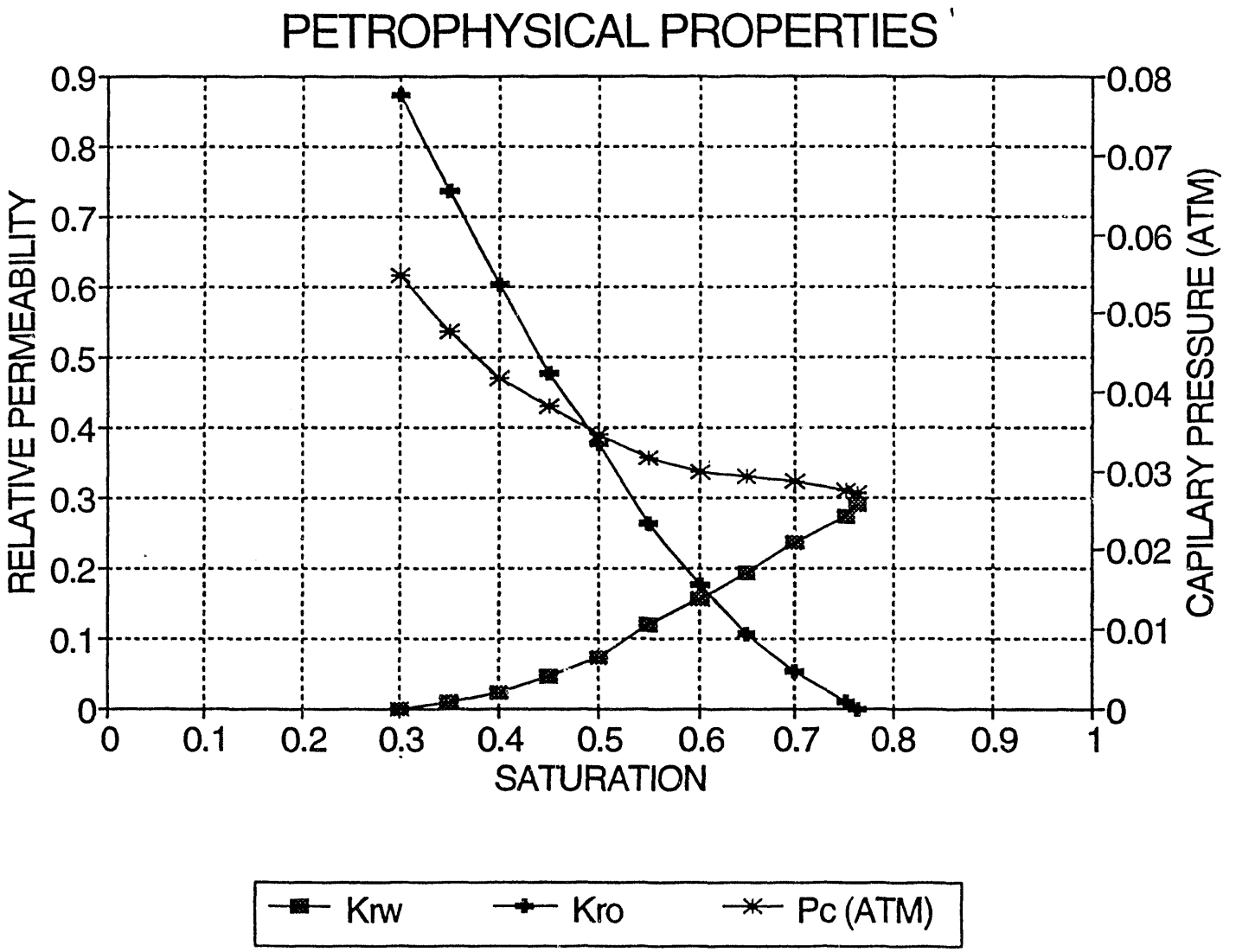
PETROPHYSICAL PROPERTIES
RELATIVE PERMEABILITY
CAPILARY PRESSURE (ATM)
SATURATION
0.9
0.8
0.7
0.6
0.5
0.4
0.3
0.2
0.1
0
0.08
0.07
0.06
0.05
0.04
0.03
0.02
0.01
0
0 0.1 0.2 0.3 0.4 0.5 0.6 0.7 0.8 0.9 1
Krw
Kro
Pc (ATM)

Figure 1

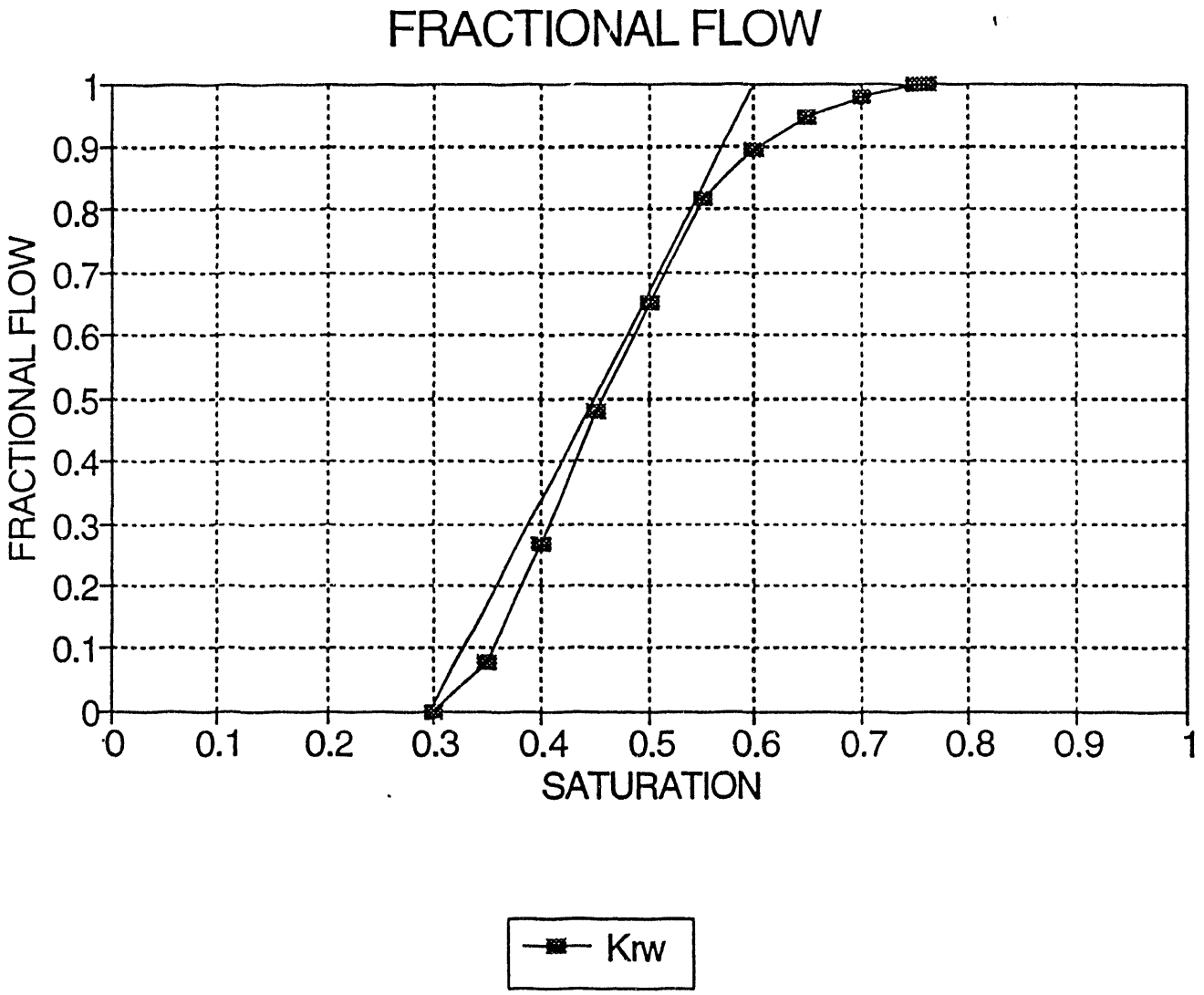
FRACTIONAL FLOW
FRACTIONAL FLOW
1
0.9
0.8
0.7
0.6
0.5
0.4
0.3
0.2
0.1
0
0
0.1
0.2
0.3
0.4
0.5
0.6
0.7
0.8
0.9
1
SATURATION
Krw

Figure 2

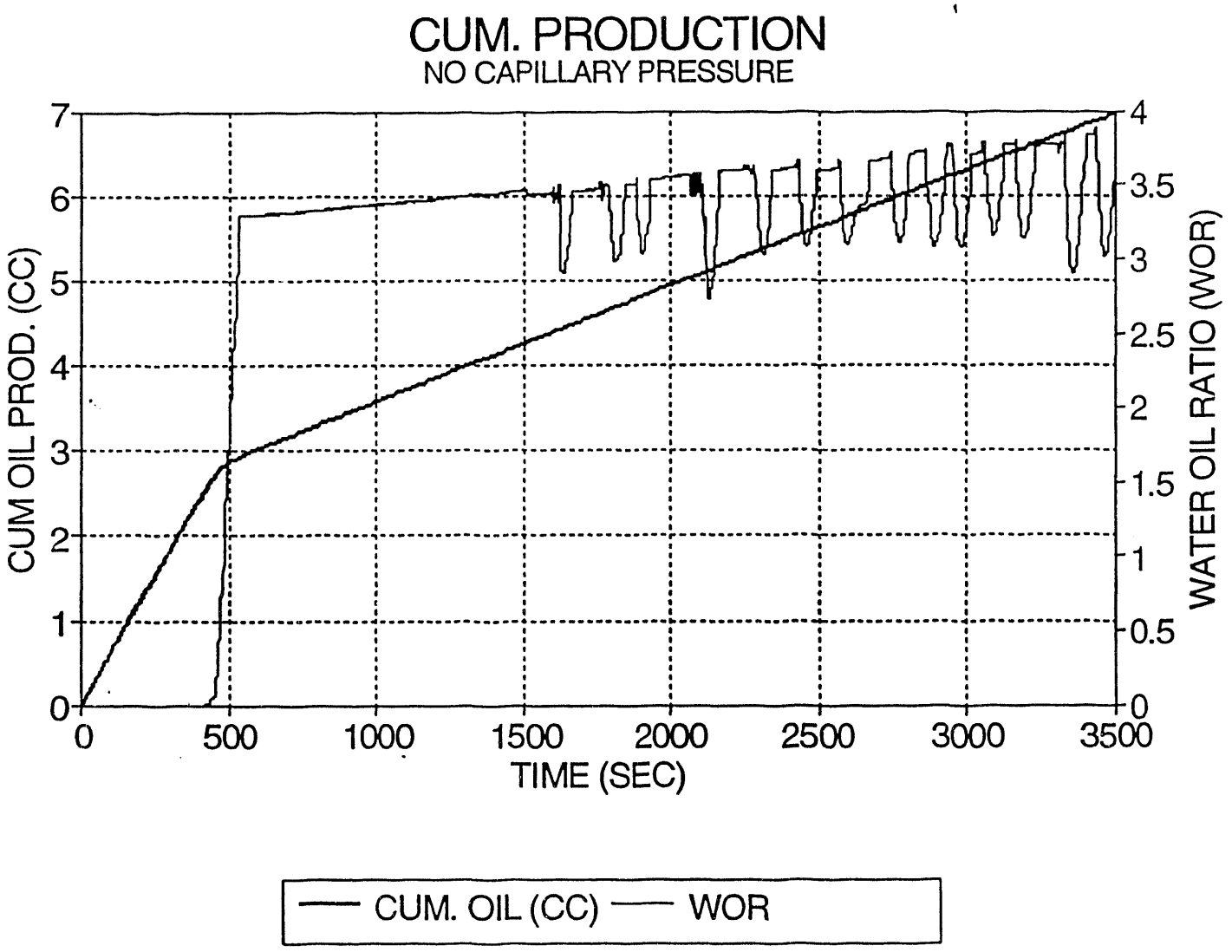
CUM. PRODUCTION
NO CAPILLARY PRESSURE
CUM OIL PROD. (CC)
WATER OIL RATIO (WOR)
TIME (SEC)
0
500
1000
1500
2000
2500
3000
3500
0
1
2
3
4
5
6
7
0
0.5
1
1.5
2
2.5
3
3.5
4
CUM. OIL (CC)
WOR

Figure 3

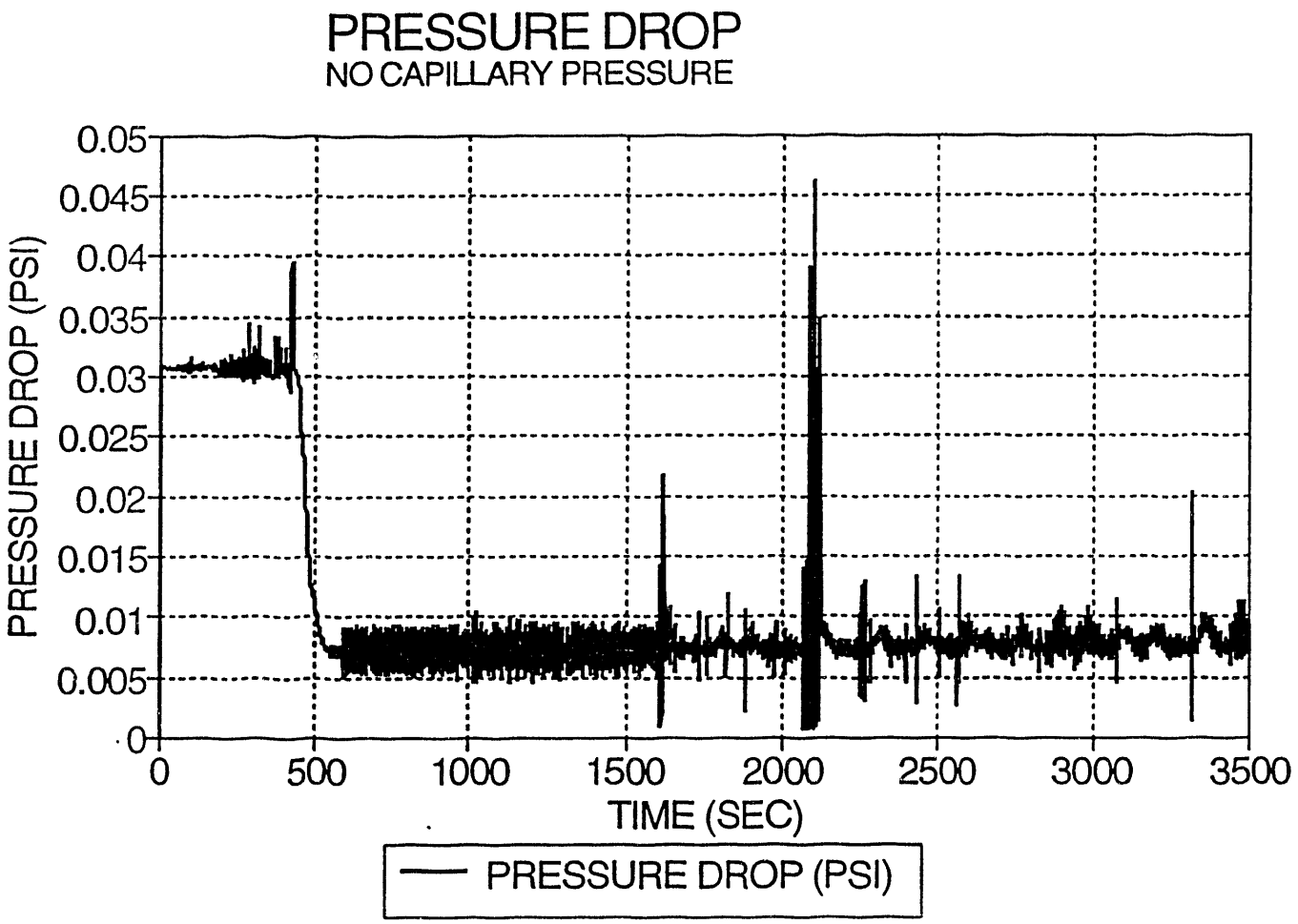
PRESSURE DROP
NO CAPILLARY PRESSURE
PRESSURE DROP (PSI)
0.05
0.045
0.04
0.035
0.03
0.025
0.02
0.015
0.01
0.005
0
0
500
1000
1500
2000
2500
3000
3500
TIME (SEC)
PRESSURE DROP (PSI)

Figure 4

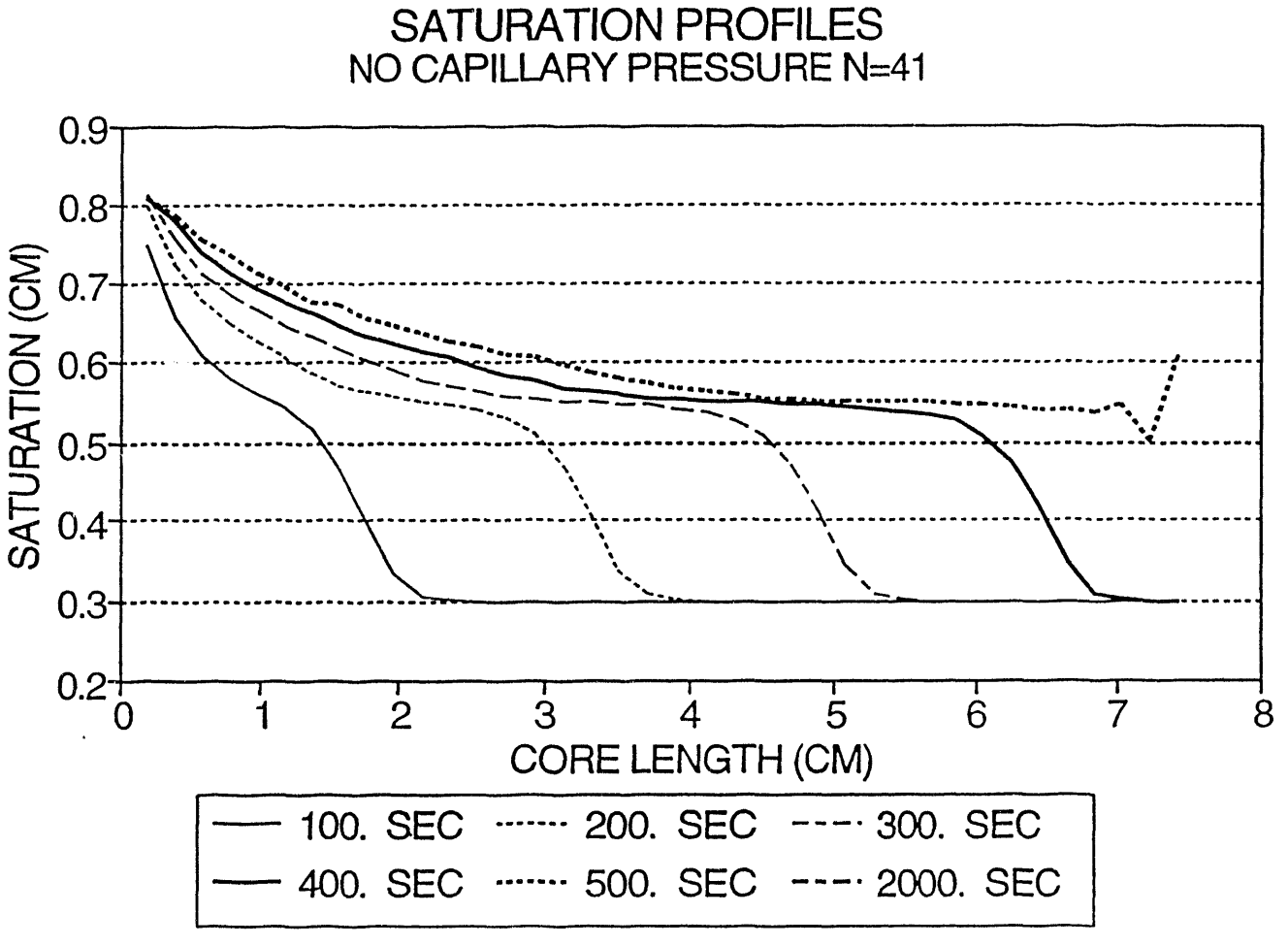
SATURATION PROFILES
NO CAPILLARY PRESSURE N=41
SATURATION (CM)
0.9
0.8
0.7
0.6
0.5
0.4
0.3
0.2
0
1
2
3
4
5
6
7
8
CORE LENGTH (CM)
100. SEC
200. SEC
300. SEC
400. SEC
500. SEC
2000. SEC

Figure 5

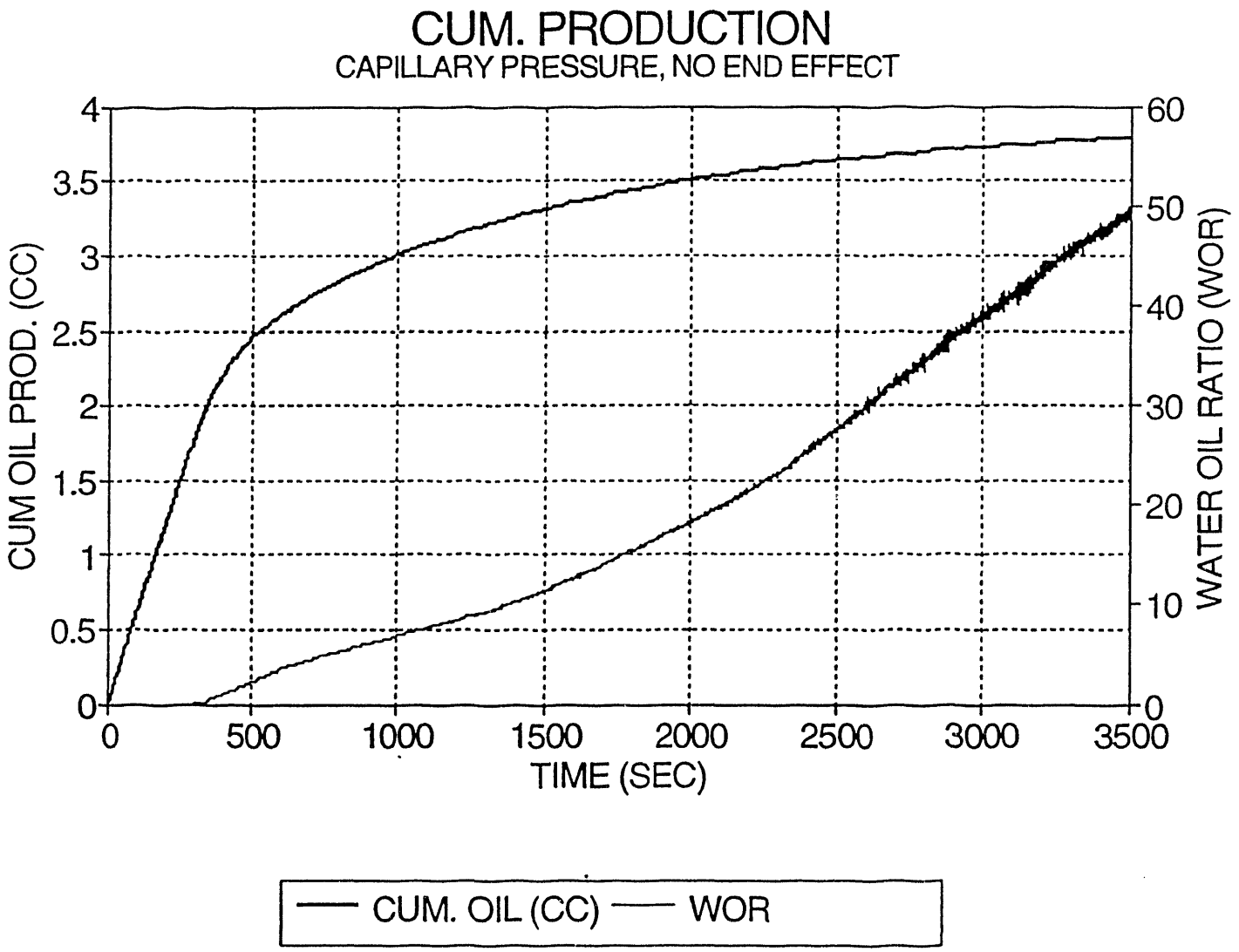
CUM. PRODUCTION
CAPILLARY PRESSURE, NO END EFFECT
CUM OIL PROD. (CC)
WATER OIL RATIO (WOR)
TIME (SEC)
0
0.5
1
1.5
2
2.5
3
3.5
4
0
10
20
30
40
50
60
0
500
1000
1500
2000
2500
3000
3500
CUM. OIL (CC)
WOR

Figure 6

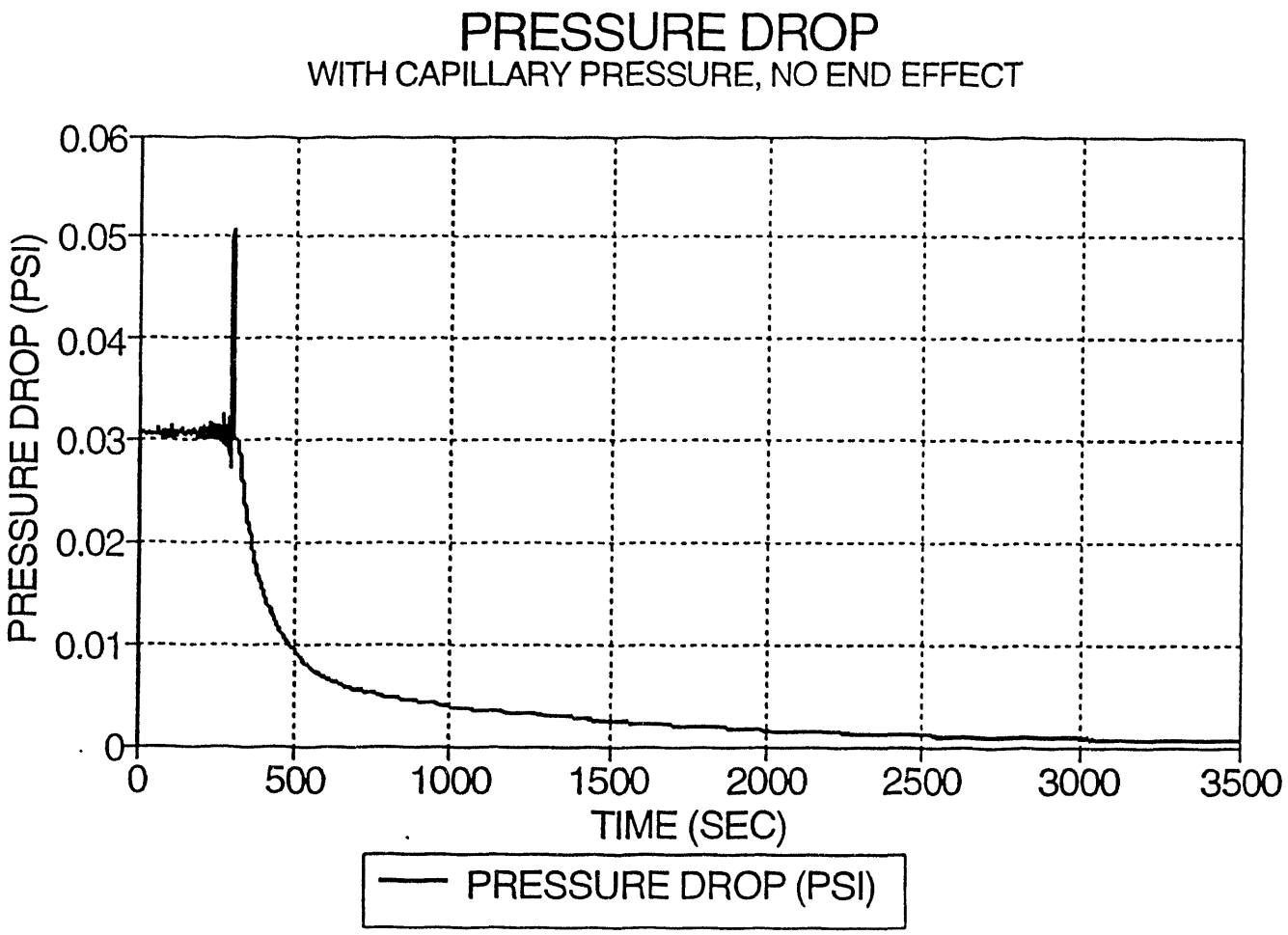
PRESSURE DROP
WITH CAPILLARY PRESSURE, NO END EFFECT
PRESSURE DROP (PSI)
0.06
0.05
0.04
0.03
0.02
0.01
0
0
500
1000
1500
2000
2500
3000
3500
TIME (SEC)
PRESSURE DROP (PSI)

Figure 7

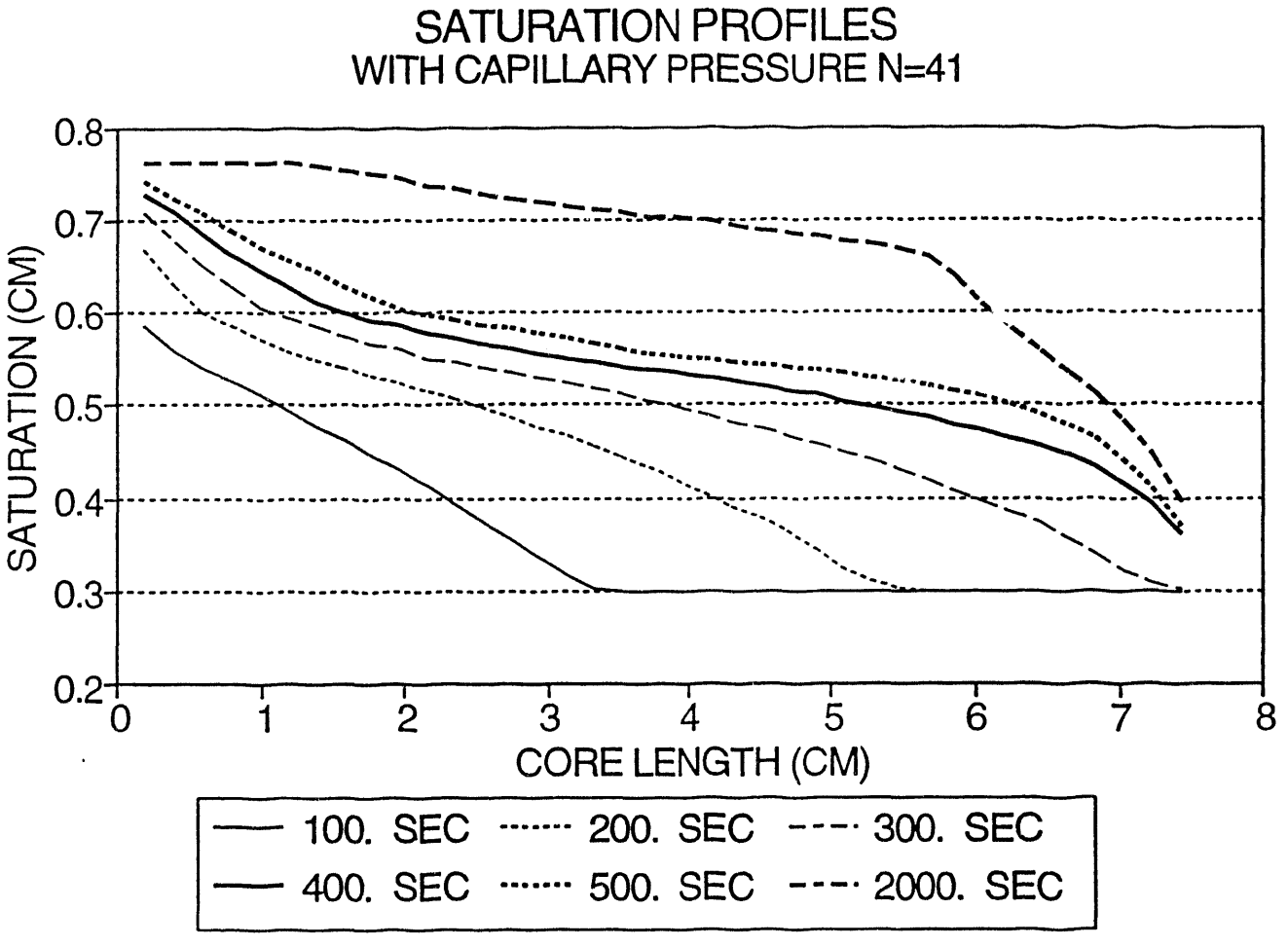
SATURATION PROFILES
WITH CAPILLARY PRESSURE N=41
SATURATION (CM)
0.8
0.7
0.6
0.5
0.4
0.3
0.2
0
1
2
3
4
5
6
7
8
CORE LENGTH (CM)
100. SEC
200. SEC
300. SEC
400. SEC
500. SEC
2000. SEC

Figure 8

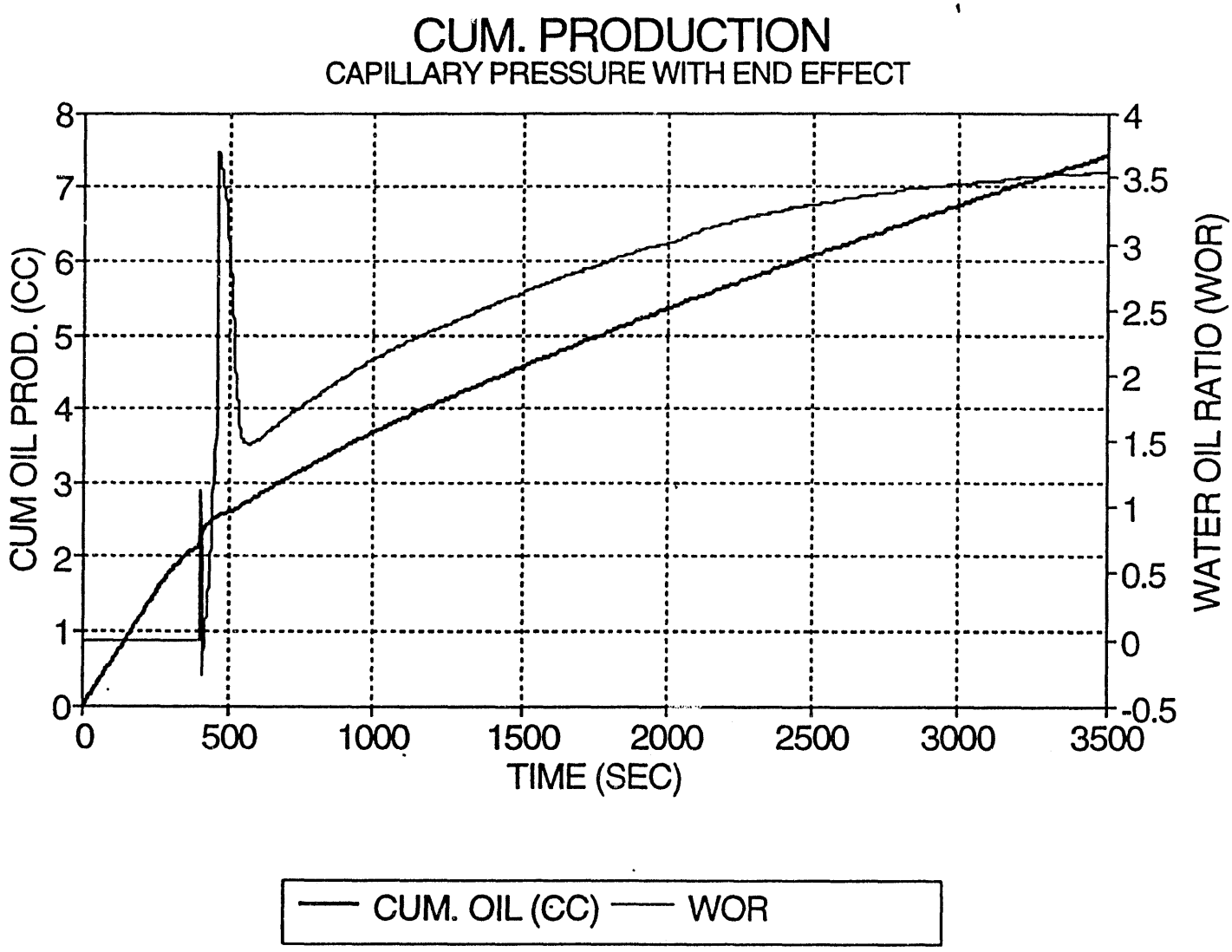
CUM. PRODUCTION
CAPILLARY PRESSURE WITH END EFFECT
CUM OIL PROD. (CC)
WATER OIL RATIO (WOR)
TIME (SEC)
0
500
1000
1500
2000
2500
3000
3500
0
1
2
3
4
5
6
7
8
-0.5
0
0.5
1
1.5
2
2.5
3
3.5
4
CUM. OIL (CC)
WOR

Figure 9

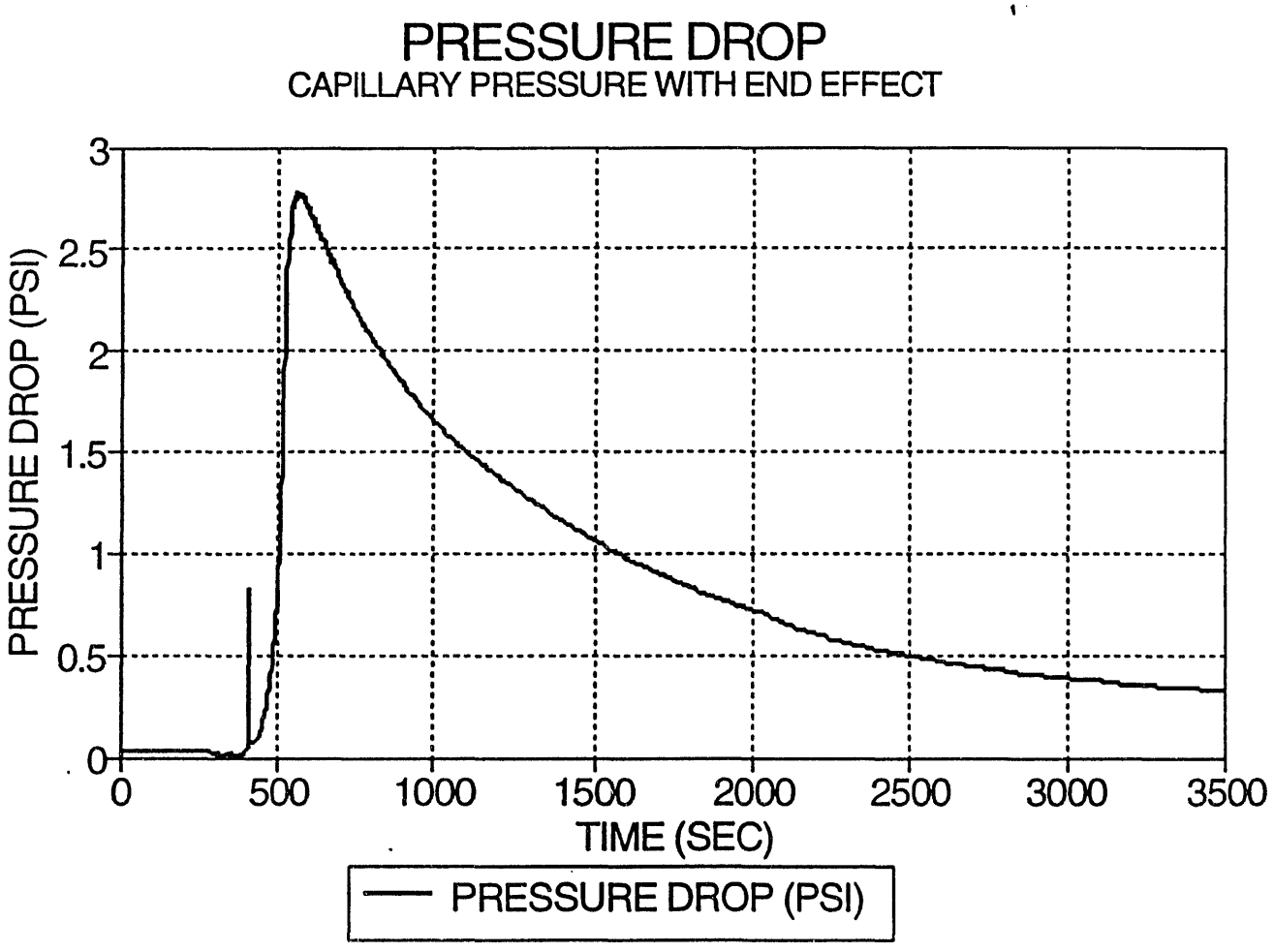
PRESSURE DROP
CAPILLARY PRESSURE WITH END EFFECT
PRESSURE DROP (PSI)
3
2.5
2
1.5
1
0.5
0
0
500
1000
1500
2000
2500
3000
3500
TIME (SEC)
PRESSURE DROP (PSI)

Figure 10

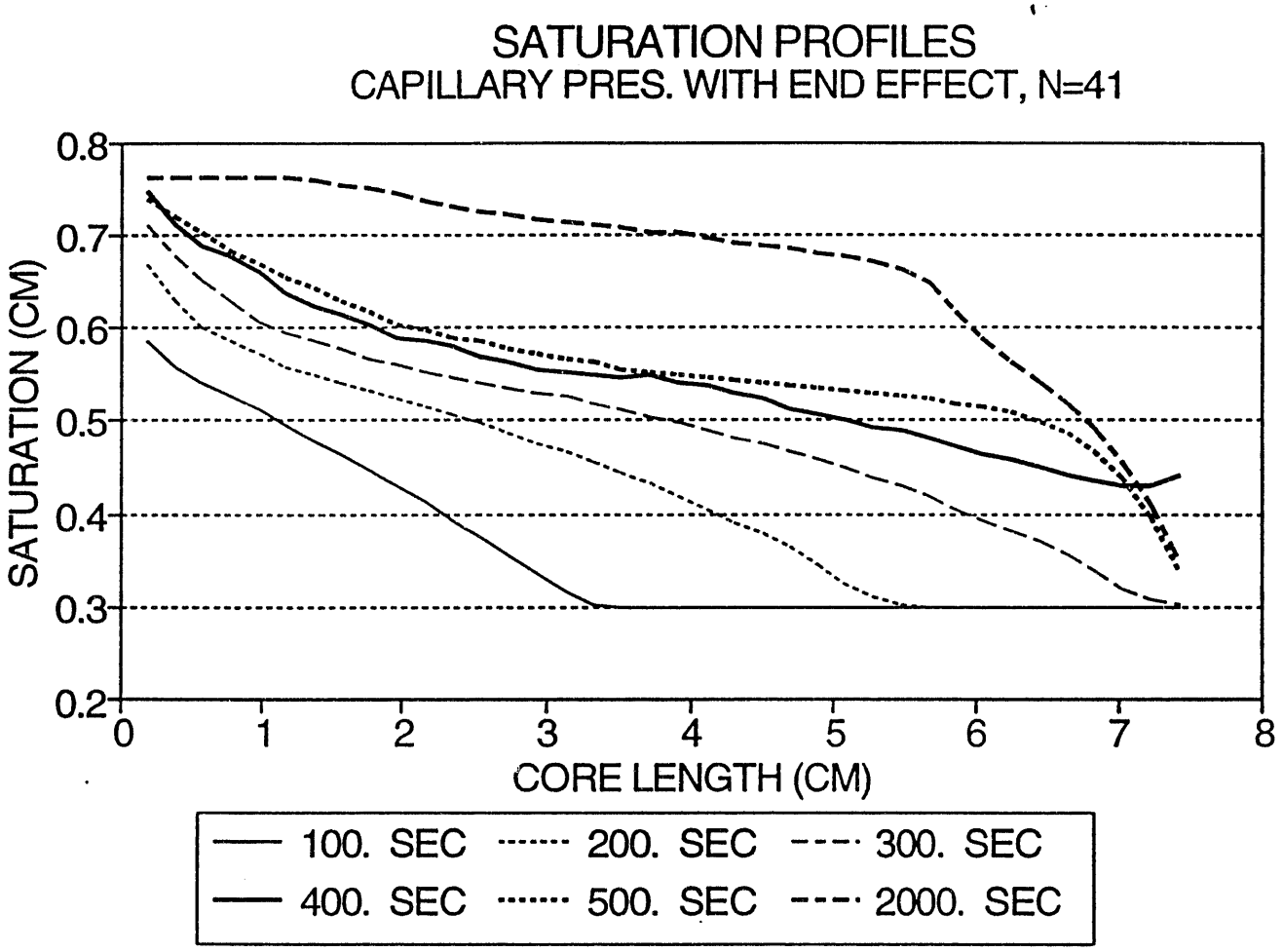
SATURATION PROFILES
CAPILLARY PRES. WITH END EFFECT, N=41
SATURATION (CM)
0.8
0.7
0.6
0.5
0.4
0.3
0.2
0
1
2
3
4
5
6
7
8
CORE LENGTH (CM)
100. SEC
200. SEC
300. SEC
400. SEC
500. SEC
2000. SEC

Figure 11

with the end-effect. The results of these two cases are shown in Table 3 and Table 4. The production history, pressure drop history and the saturation history profiles are given in Fig. 6-11, respectively.

A new feature is in the process of being added to the two phase flow simulator while conducting the test runs. A non-linear optimization IMSL routine will be incorporated into the simulator in an attempt to obtain the same relative permeability and capillary pressure curves.

DIMENSIONAL ANALYSIS AND CORRELATION OF EXPERIMENTAL DATA

To date 1800 non-Darcy flow experimental data points have been collected and cataloged . In an attempt to identify a dimensionally consistent correlation which relates the non-Darcy flow coefficient to rock and fluid properties the following approach was pursued using dimensional analysis:

$$\pi_i = f_i(Q_i, R_e, \phi(1-S)) \tag{1}$$

In equation 1 π_i are dimensionless groups involving the non-Darcy flow coefficient (β), Q_i are dimensionless groups which do not involve β, and R_e is the Reynolds number, ϕ is the rack porosity and S is the liquid saturation.

The dimensional groups π_i and Q_i which were identified for further analysis are:

$$\pi_1 = \beta\sqrt{k_e}, \quad \pi_2 = \rho V/\mu\beta, \quad \pi_3 = \sigma/\beta\mu V, \quad \pi_4 = \sqrt{\rho\sigma}/\mu\beta$$

$$Q_i = R_e\sqrt{\phi}, \; Q_2 = \sigma/\rho V^2, \; Q_3 = \rho\sigma k_e/\mu^2, \; Q_4 = \sigma^2 k_e/\mu V^2 \tag{2}$$

In the expressions for π_i and Q_i, k_e is the effective phase permeability, V is the fluid phase velocity, ρ is the phase density, μ is the phase viscosity and σ is the effective stress.

Using a multiple linear regression technique an expression of the form shown in equation 3 is sought which gives the best fit to the experimental data.

$$\pi_i(1-S)\phi = a_0 Q_i^{a1} Q_j^{a2} \tag{3}$$

Some errors were discovered in the original regression analysis so we are in the process of re-doing the calculations to remove these errors. Hopefully we will be able to identify a correlation which is more general and accurate than has been published to date using this technique.

NON-DARCY FLOW LABORATORY STUDIES

The following tasks have been completed in the Non-Darcy Flow Studies Laboratory.

1. Upgrading of the Non-Darcy Flow Apparatus - This earlier work included installing new fittings (some were heat damaged), pressure testing, and calibration. This work was

necessary for the data acquisition phase which followed.

2. Acquisition of Data for the "Sensitivity of the Non-Darcy Flow Coefficient to Core Length Investigation" - Non-Darcy flow data was obtained to study on the effects of varying the total flow path length of the core sample against the value of non-Darcy Flow coefficient (and effective permeability) to determine a "characteristic value" as the core length approaches zero. Typical flow data are presented in Table 4.

3. The Non-Darcy Flow (Computer Analog) Remote Control/Automated Data Acquisition System Upgrade Phase - The design of the upgraded equipment are given schematically in Figures 12 and 13.

4. Fabrication of the API Proppant Cell - An API Proppant flow cell apparatus was to be used to examine the non-Darcy flow effect in propped hydraulic fractures (see Figures 14 and 15, and the attached photographs). The pump, hydraulic fluid reservoir, and hydraulic press were all donated by Occidental Petroleum. Its features include:

   A. Complete compatibility with the (previously existing) non-Darcy flow apparatus (which utilizes a Hassler-Sleeve type coreholder), utilizing quick connects for rapid crossover. This system ties in with the automated (analog) data acquisition system which was previously described (in part 3 above).

   B. Direct determination of the dynamic fracture width during testing utilizing LVDT's, with automatic data acquisition.

   C. Direct determination of the applied load during testing utilizing a load cell, also with automatic (analog) data acquisition.

   D. Engineered to handle fluid temperature up to 250°F during high-temperature flow studies.

Some problems have been encountered with the experimental research program due to equipment malfunctions, inappropriate data acquisition software, and design refinements which needed to be incorporated into the experimental apparatus to make it safer. These minor modifications have consumed a considerable amount of time but are essentially completed at this stage of the project. These modifications will permit us to perform single and multiphase non-Darcy flow experiments in a more rapid and efficient manner.

Research Papers Prepared from the Project

Several research papers have been prepared or are in the process of being prepared for submission to referred journals and/or Society of Petroleum Engineers Technical Conferences. The titles of these papers are:

1) Detailed Interpretation of the Non-Darcy Flow Parameters Via An Alternative Derivation

Table 4. Sensitivity of the Non-Darcy Flow Factor to Core Length Investigation Data

(in) Core Length	Run #	(1/cm)	($1/cm^2$) Intercept	(md) Permeability
4.0	1	7.38 E05	7.00 E08	147.4
	2	8.10 E05	6.85 E08	150.6
	3	7.80 E05	7.00 E08	147.4
3.0	1	7.65 E08	7.15 E08	141.8
	2	7.80 E05	7.00 E08	147.4
	3	8.05 E05	6.90 E08	146.8
2.0	1	8.10 E05	7.40 E08	136.9
	2	8.36 E05	7.38 E08	137.3
	3	8.04 E05	7.48 E08	135.5
1.0	1	9.80 E05	7.65 E08	132.5
	2	9.58 E08	8.10 E08	125.1
	3	10.16 E08	7.82 E08	129.6

Figure 12. Non-Darcy Flow Apparatus Schematic, Section 1 (by Ed Evans, 3/11/92)

Figure 13. Non-Darcy Flow Apparatus Schematic, Section 2 (by Ed Evans, 3/11/92)

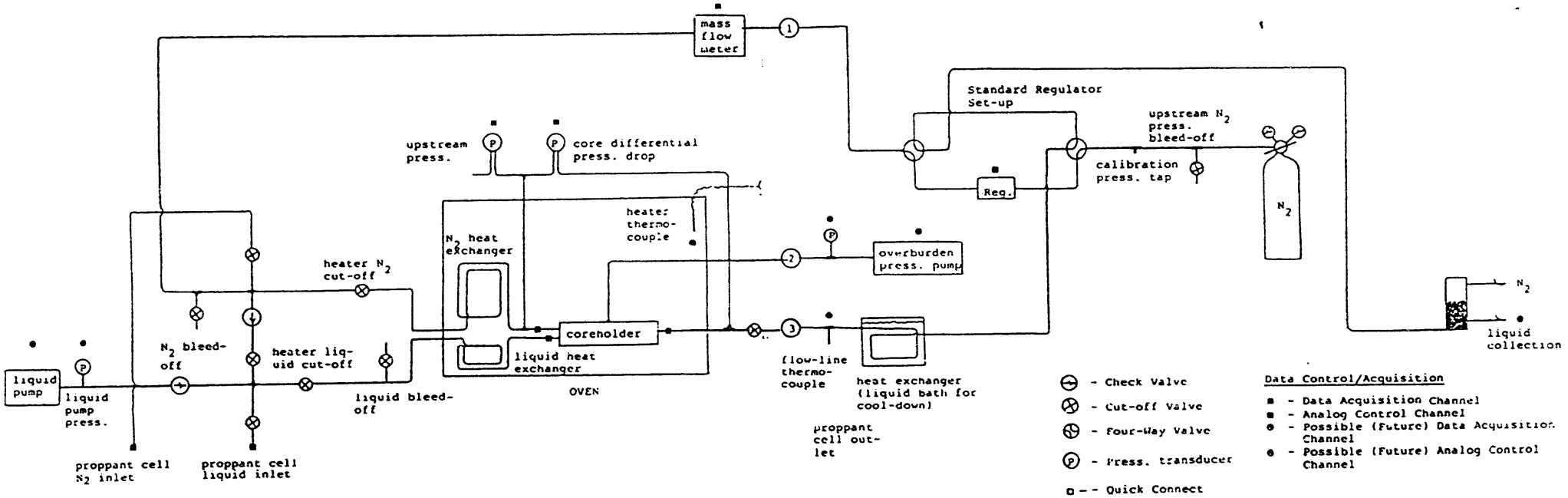

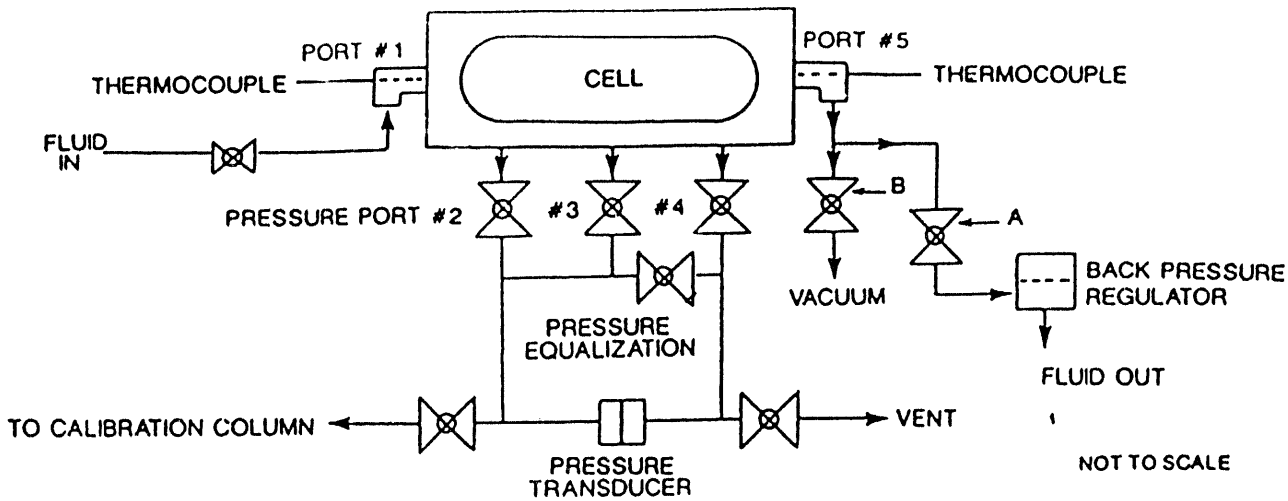

FIG. 14
SCHEMATIC OF FLOW PATHS THROUGH
THE API PROPPANT PACK CONDUCTIVITY TEST UNIT

Courtesy of the Western Company

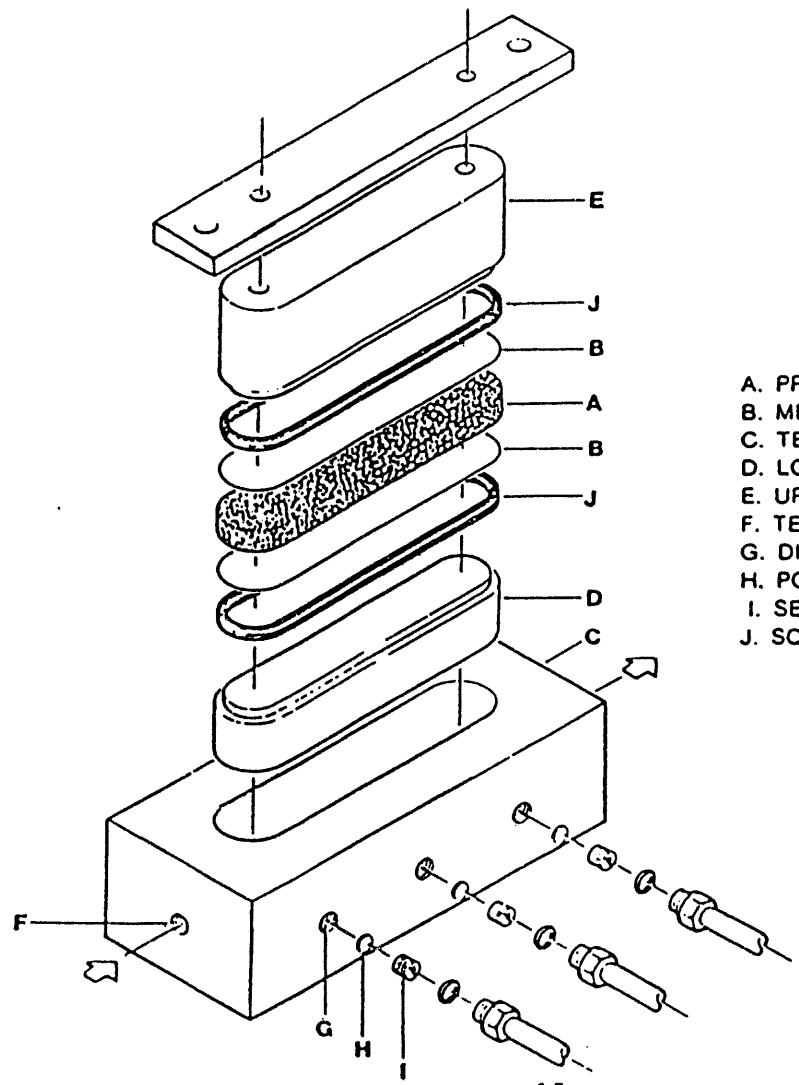

A. PROPPANT PACK 7 INCH × 1.5 INCH × W_i
B. METAL PLATEN
C. TEST UNIT BODY
D. LOWER PISTON
E. UPPER PISTON
F. TEST FLUID ENTRY/EXIT PORT
G. DIFFERENTIAL PRESSURE SENSING PORT
H. POROUS METAL FILTER
I. SET SCREW
J. SQUARE RING SEAL

NOT TO SCALE

FIG. 15
EXPLODED SCHEMATIC DIAGRAM OF
API PROPPANT PACK CONDUCTIVITY TEST UNIT

Courtesy of the Western Company

DOE Non-Darcy Flow Characterization Project API Proppant Cell (Fabricated by Ed Evans, 3/15/92)

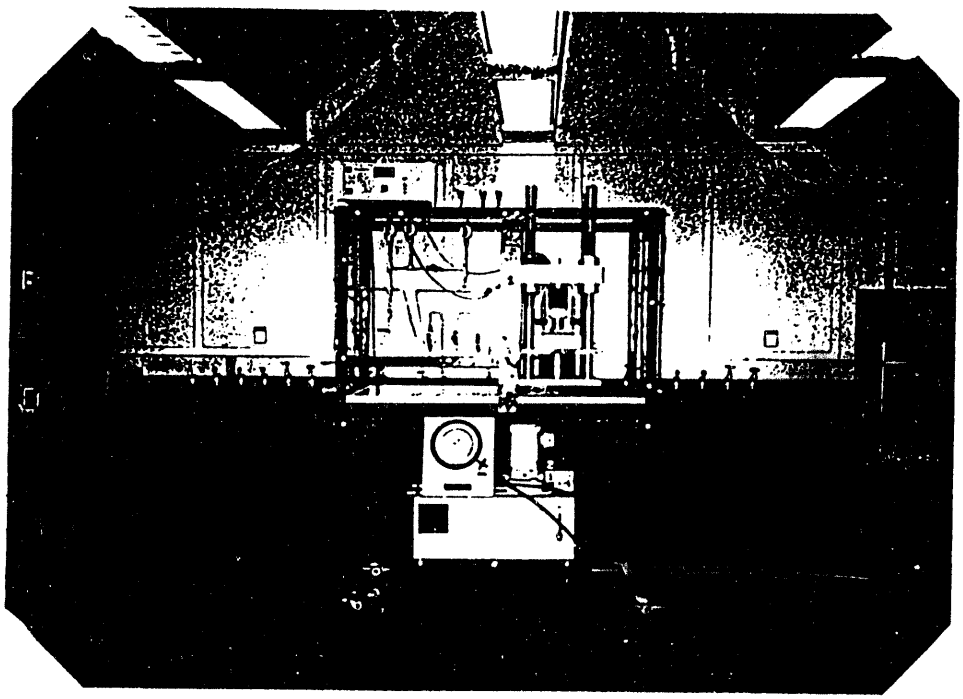

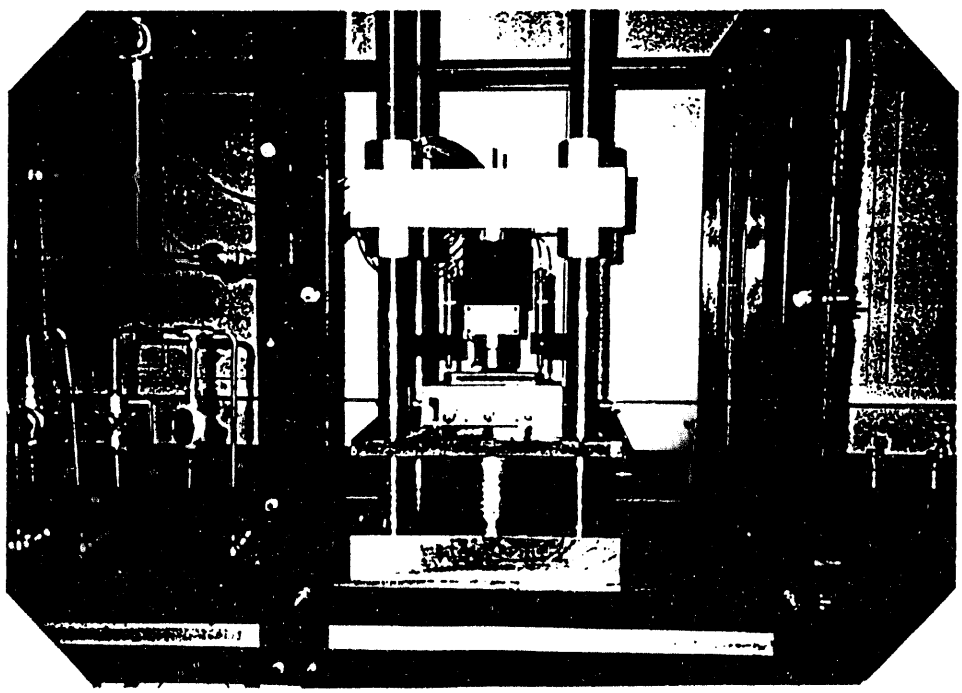

of the Porous Media Momentum Equation

2) Modification of the JBN Method for the Effects of Interfacial Drug and Inertial Flow

3) Generalized Correlation for Non-Darcy Flow Parameters at Reservoir Conditions

4) Simulated Annealing for Relative Permeability and Capillary Pressure from Unsteady State Non-Darcy Displacements

5) Direct Analytical Method for Simultaneous Determination of Relative Permeabilities and Capillary Pressure for Non-Darcy Flow of Gas/Brine Systems

RESEARCH PLANS FOR 1992-93

During the third and final year of the project, efforts will be directed toward utilizing the multi-phase flow numerical model to predict the two phase non-Darcy flow coefficients, relative permeabilities, capillary pressures, and the interfacial drag between phases from basic flow measurements for gas/liquid systems.

Effort will also continue toward identifying the most appropriate dimensionless correlations which will describe the non-Darcy flow coefficient as a function of rock and fluid properties.

Finally, effort will also by directed toward completing the experimental aspects of the project. The experimental program will focus upon developing a systematic method for measuring the non-Darcy flow coefficient under multi-phase flowing conditions.

In addition, the experimental program will provide basic flow measurement data in support of the theoretical mark and the dimensional analysis and correlation research.

THE UNIQUE VALUES ARE:

4	*Contains proprietary information
1	ABC Laboratories, Inc.
2	AccSys Technology, Inc.
1	Acid Rain Control, Inc.;Kurchatov Institute (Russian Science
1	Acteron Corp.
1	Advanced Ceramics Research, Inc.
1	Advanced Fabrications, Barnes Aerospace
2	Advanced Micro Devices, Inc.
1	Advanced Refractory Technologies Inc.
1	Advanced Research Development, Inc.
2	AECL Technologies, Inc.;Applied Poleramic, Inc.;Boeing Co.,
1	Aerojet-General Corp., Electronic Systems Div.
1	Aeternum Corp.
2	Air Products and Chemicals, Inc.
1	Airotech, Inc.
2	Aladdin Industries, Inc.
1	Alaska Dept. of Community and Regional Affairs, Div. of Ener
1	Alcan International Limited
2	Alliant Techsystems, Inc.
1	Allied Signal, Inc.
1	Allied-Signal Aerospace Co., Garrett Ceramic Components Div.
3	Allied-Signal, Inc.
1	Allied-Signal, Inc., Research and Technology
1	Alpha Industries, Inc.
1	Alternative Fluorocarbon Environmental Acceptability Study (
4	Aluminum Co. of America
1	Aluminum Recycling Association
1	AMAX Coal Industries, Inc.
1	AMAX Plating, Inc.
1	American International Technologies, Inc.
1	American Society for Testing and Materials
2	Amgen, Inc.
1	Amoco Chemical Co.
4	Amoco Corp.
1	Amoco Corp.; Chevron-Conoco Shale Oil Semiworks Joint Ventur
1	Amoco Corp.;Bio-Imaging Research Inc.
1	Amoco Oil Co.
4	Amoco Oil Co., Research and Development Dept.
1	Ampex Corp.
1	Analog Devices, Inc.
1	Analysis Programming Processing Instrumentation
1	Anderson Labs.
2	Appliance Research Consortium, Inc.
1	Applied Biosystems, Inc.
1	Applied Materials, Inc.
1	Argonne National Laboratory;Otter Tail Power Co.;Green Isle
1	Astex Applied Science and Technology, Inc.
1	AstroPower, Inc.
7	AT and T Bell Labs.
1	AT and T Co.
1	AT and T Co.;Eveready Battery Co.;Rayovac Corp.;Wilson Great
1	AT/Scan Ltd.
1	Atlanta Gas Light Co.;Public Service Co. of North Carolina,
1	Aurora Technologies, Inc.
1	AVX Tantalum Corp.
1	B and W Nuclear Co.;Duke Power Co.
4	Babcock and Wilcox Co.
1	Basic Aircraft Research Corrosion Facility
1	Baxter Healthcare Corp.
1	Baxter International, Inc.
1	BE Software Co.
2	Beckman Instruments, Inc.
1	Beckman Laser Institute and Medical Clinic

DATE

FILMED

6/14/94

END